RECENT PROGRESS ON CO-BASE ALLOYS: PHASE DIAGRAMS AND APPLICATION

K. Ishida[1]

Abstract

This paper presents recent progress on the phase diagrams and design for Co-base alloys, focusing on magnetic recording media, ferromagnetic Co-Ni-Al-base shape memory alloys and Co-base superalloys. The calculated miscibility gap between ferromagnetic and paramagnetic states in the Co-X(X: Cr, Mo, W) systems was found to agree well with the experimental results, strongly implying that the magnetic induced phase separation is responsible for the compositional heterogeneity in Co-base magnetic recording media. New ferromagnetic Co-Ni-Al shape memory alloys were also developed based on phase diagrams. The introduction of γ(Al structure) to the β(B2) matrix was found to drastically improve the ductility. Finally, the possibility of potent strengthening of Co-base superalloys upon precipitation of γ'(L12) phase is presented.

Key words: Magnetic recording media; Ferromagnetic shape memory alloy; Co-base superalloy

[1] *Technical contibution to 62nd ABM - International Annual Congress, July 23rd to 27th, 2007, Vitória - ES – Brazil*

[2] *Professor, Department of Materials Science, Tohoku University, Aoba-yama 6-6-02, Sendai 980-8579, JAPAN*

1. Introduction:

Cobalt-base alloys are widely used in various applications such as magnetic materials, corrosion and heat-resistant alloys, wear-resistant alloys, prosthetic alloys in medical parts etc., where the phase diagrams play a key role in material development.

In this paper, the research activities of phase diagrams and applications for Co-base alloys in our laboratory have been presented, focusing on the following alloy systems.

(1) Experimental and thermodynamic calculations on phase diagrams of Co- (Cr, Mo, W) base alloys for magnetic recording media[(1)~(7)].
(2) Phase diagram and microstructural evolution of Co-Ni-Al ferromagnetic shape memory alloy[(8)~(14)].
(3) Phase stability of half-metal-type Co-Cr base Heusler alloys[(15)~(21)].
(4) Co-base superalloys with γ + γ' structure[(22), (23)].

2. Co-base Magnetic Recording Media:

Co-Cr-based sputtered films are in the current of high-density longitudinal magnetic recording media, and also promising materials for perpendicular magnetic recording media. The Co-Cr-based film is made up of Co-rich ferromagnetic hexagonal-closed-packed (hcp) nanosized grains surrounded by a Co-poor paramagnetic hcp phase. This unique compositional modulation weakens the interparticle exchange interaction between the ferromagnetic grains, resulting in improvements of recording resolution as well as significant recording noise reductions. Such a compositional modulation due to the magnetically induced phase separation in a hcp phase is easily developed during the thin-film growth process on heated substrates around at 500-700K. The magnetically-induced phase separation is also confirmed in the Co-W binary system by diffusion couple method. Figure 1 shows the calculated phase diagram of Co-W binary system compared with experimental data. Based on the results, a nanoscale compositional fluctuation caused by magnetically induced phase separation was also confirmed in the films deposited on a heated substrate in analogy with Co-Cr based alloys as shown in Fig.2.

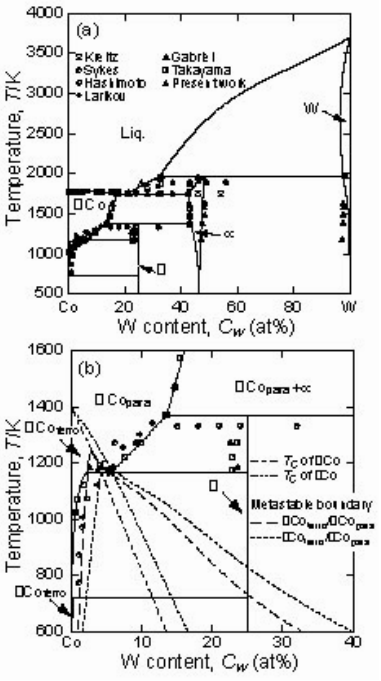

Fig.1 Calculated phase diagram of the Co-W system: (a) whole system, (b) Co-rich corner including the metastable phase boundaries

Figure 3 shows the in-plane magnetization curves of the films measured along NaCl [110] direction. The relatively large value of Hc for the film is associated with a large value of magnetocrystalline anisotropy materials. Consequently, the Co-W sputtered films as well as the Co-Mo films are promising as next generation high-density magnetic recording media.

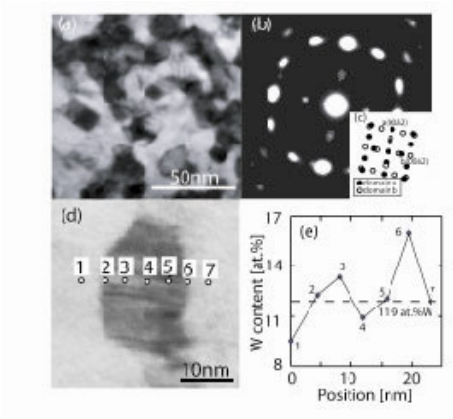

Fig. 2 Several kinds of data for Co-11.9 at% W film deposited at 573 K:
(a) TEM bright-field image,
(b) the corresponding SAD pattern,
(c) the indexed-electron-diffraction pattern,
(d) STEM bright-field image, and
(e) the local composition at the numbered positions.

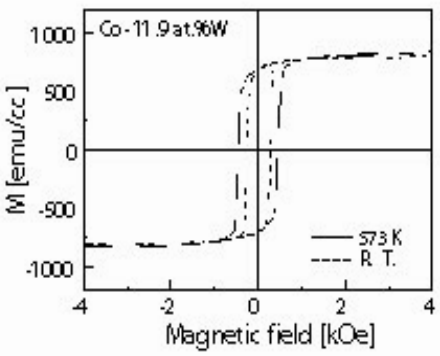

Fig. 3 Magnetization curves of Co-11.9 at% W films deposited at room temperature and at 573 K.

3. Co-Ni-Al Ferromagnetic Shape Memory Alloys:

Ferromagnetic shape-memory alloys (FSMAs) have received much attention as high-performance magnetically controlled actuator materials because they show a large magnetically induced strain by the rearrangement of twin variants in the martensite. Several candidates for FSMAs have been reported, including Ni_2MnGa, Fe-Pd, and Fe_3Pt alloys. Recently, the authors found a new group of FSMAs in Co-Ni-Al β (B2 structure)-based alloys.

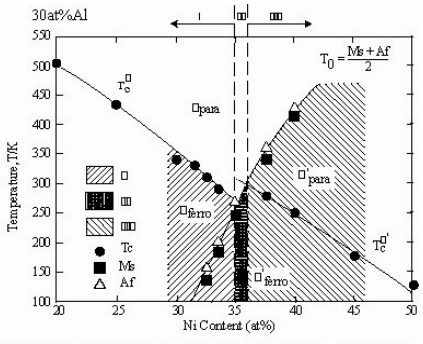

Fig. 4 The compositional dependence of the Curie temperature (Tc), the martensitic transformation temperature (Ms), and the austenite fonishing temperature (Af) in $Ni_{70-x}Co_xAl_{30}$ alloys.

The Curie temperature (Tc), the martesitic transformation starting temperature (Ms), and the reverse-transformation finishing temperature (Af) are plotted as a function of the Co content in the 30 at.% aluminum section, as shown in Fig. 4. The alloys show thermoelastic martensitic transformation from the β to β' ($L1_0$ structure) accompanied by the shape-memory effect. Ms increases and Tc decreases with increasing Ni

content. The phase-transformation behavior of the alloys on cooling can be grouped into three types based on the characteristic features of the magnetic and martensitic transformations. In Type I, the paramagnetic β phase is magnetically transformed into the ferromagnetic β phase, and then martensitically transformed into the ferromagnetic β' phase (i.e., $T_C^{\beta} > Ms$). In Type II, the paramagnetic β' phase is directly transformed into the ferromagnetic martensite β' phase (i.e., $T_C^{\beta} < Ms < T_C^{\beta'}$). In Type III, the paramagnetic β phase is martensitically transformed into the paramagnetic β' phase and eventually ferromagnetic transition occurs in the β' phase (i.e., $T_C^{\beta'} < Ms$). In the case of Type I alloys, the magnetization drastically increases and decreases at As and Ms temperatures, respectively. A large magnetocrystalline anisotropy energy of $Ku=3.9*10^6$ erg/cm^3 was confirmed in the martensite phase of the Co-Ni-Al β single crystal, being the same order of that of Ni_2MnGa. In the case of Type II alloys, the magnetization drastically decreases and increases at As and Ms temperatures, respectively. This is due to the difference in the Curie temperature between the β and β' phases.

The presence of the fcc-γ solid solution as a second phase in the NiAl-β-based alloy system rendered the alloy ductile and developed β+γ two-phase shape-memory alloys in the NiAl-β-based system including Fe, Co and Mn. The contours of iso-Ms and iso-Tc lines drawn on the basis of the experimental data are shown in Fig. 5 together with the phase boundaries of β+γ at 1100℃ and 1300℃ of the Co-Ni-Al ternary system. The composition range of the β-phase alloy exhibiting the FSME is located near the β+γ two-phase boundary. The β+γ two-phase FSMAs can be produced by a suitable choice of alloy composition and annealing temperature. The $Co_{40}Ni_{33}Al_{27}$ alloy was investigated as a typical β+γ two-phase FSMA. The ductility of the alloy can be significantly improved by the introduction about 7vol% γ phase, as reported other NiAl-β-based alloys, although the β single–phase polycrystalline alloys, as well as the Ni_2MnGa show poor ductility. The shape-memory effect in the ferromagnetic state of the β+γ two-phase FSMA was examined by a simple bending test. A 150 μm thick specimen of the two-phase alloy was annealed at 1350 ℃ for 2 min. and at 1300℃ for 15 min. The thin plates were bent to realize a surface strain of 2% at Ms (-13℃). Upon heating above Af to 26 ℃, shape recovery of about 83% was obtained.

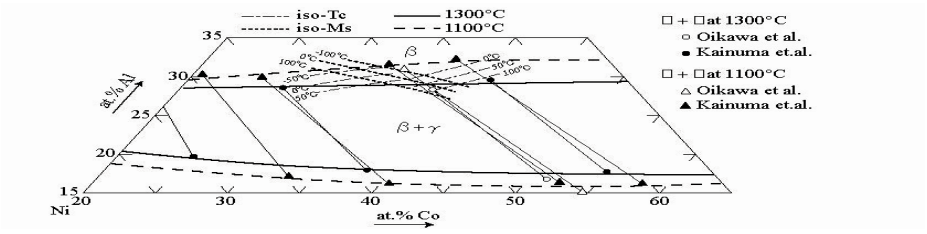

Fig. 5 The Tc and Ms temperatures related to the phase Diagram of Ni-Al-Co ternary system.

4. Phase Stability and Half-metallic Properties of Co-Cr base Heusler Alloys:

Half-metallic ferromagnets (HMFs) are currently interesting in the field of spintronics in order to realize spin-dependent devices with high performance, and many $L2_1$ (full-Heusler)-type HMFs have been extensively studied from both theoretical and experimental viewpoints. Recent band calculations have shown clear evidence for the HMFs from the electronic structures of $L2_1$ and B2-type Co_2CrAl alloys. However, experimental values of the saturation magnetic moment, Ms, and the spin polarization of the $L2_1$ and B2-type Co_2CrAl alloys are much lower than the theoretical values. Recently, we have demonstrated that an inevitable A2 + B2 spinodal decomposition which appears in the Cr-rich portion of $Co_2Cr_{1-x}Fe_xAl$ alloys significantly reduces the half-metallic magnetic properties. Since half-metallic properties including spin polarization strongly depend on the crystal structure and the degree of order, detailed information on the phase stability is useful for realizing HMF characteristics.

The phase stability of Co-Cr-Ga and Co-Cr-Fe-Ga Heusler alloys were investigated. Figure 6 shows the vertical section diagram of 50 at%Co in Co-Cr-Ga ternary system. The temperatures of T_c and the $T_t^{B2/L21}$ increase with the Ga content, and the maxima of T_c and $T_t^{B2/L21}$ are converged to the stoichiometric content of Co_2CrGa. It is also shown that the measured $T_t^{B2/L21}$ curve is in good agreement with the Bragg-Williams-Gorsky (BWG) approximation, where the calculated $T_t^{B2/L21}$ is described by a parabolic curve as a function of atomic content, and the maximum $T_t^{B2/L21}$ is at the stoichiometric (Co_2CrGa) composition. Consequently, the $L2_1$-type single-phase alloys in the Co-Cr-Ga system can be easily obtained by quenching, in contrast to the Co-Cr-Al alloy system which exhibits an inevitable A2 +B2 spinodal decomposition.

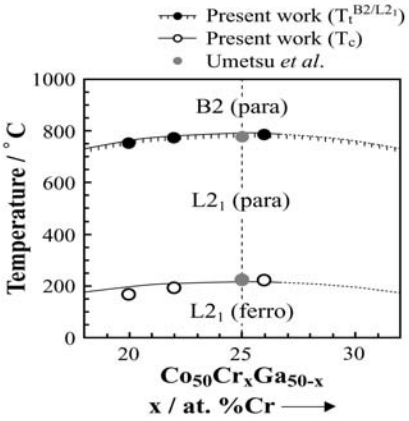

Fig. 6 Vertical section diagram of 50 at% Co in the Co-Cr-Ga ternary system, together with the previous experimental data.

Figure 7 shows a metastable phase diagram of the $Co_2Cr_{1-x}Fe_xGa$ alloy system, together with data on the $Co_2Cr_{1-x}Fe_xAl$ alloy system. The bold hatched and dotted lines represent the transition temperature from the $L2_1$-to B2 type phase $T_t^{B2/L21}$ and the Curie temperature T_c, respectively, determined by the DSC measurements. The transition temperature from the $L2_1$-to B2 type phase $T_t^{B2/L21}$ is 1082 ±13K, about 150K higher than that of the $Co_2Cr_{1-x}Fe_xAl$ system, and the Curie temperature T_c monotonically increases with increasing x. It is also revealed that the $L2_1$-type single-phase can be easily obtained in the entire range of x for the $Co_2Cr_{1-x}Fe_xGa$ system, in contrast to the $Co_2Cr_{1-x}Fe_xAl$ system in the Cr-rich portion which exhibits a

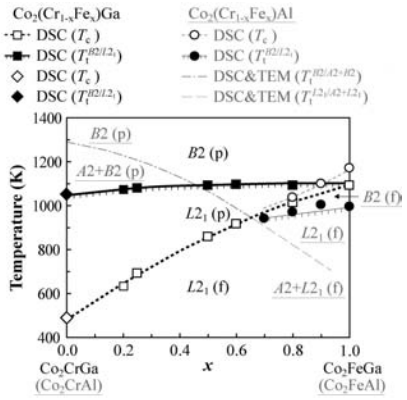

Fig. 7 Metastable phase diagram of the $Co_2Cr_{1-x}Fe_xGa$ alloy system compared with that of the $Co_2Cr_{1-x}Fe_xAl$ system.

spinodal decomposition from the B2 to A2 +B2 phase and from the $L2_1$ to A2 + $L2_1$ phase in the higher and lower temperature range, respectively.

Based on these results, the concentration dependence of the spin polarization ratio *P* (%) for the $L2_1$-and B2-type $Co_2(Cr_{1-x}Fe_x)Ga$ alloy systems is shown in Fig. 8. The value of P becomes smaller with increasing x, and the value of B2-type phase is lower than that of the $L2_1$-type phase in the entire concentration range of x. Especially, in higher concentration of x, the difference between P in both the phases becomes significant. For x = 1.00 (≡Co_2FeGa), the ratio of P for the $L2_1$-type phase is 37%, resulting in a remarkable reduction of a half-metallic property. For practical applications, the half-metallic ferromagnets having a high spin polarization ratio P with a high Curie temperature T_c are highly desired. Accordingly, high values of the spin polarization ratio and the Curie temperature are obtainable by adjusting the amount of Fe for Cr in the $Co_2(Cr_{1-x}Fe_x)Ga$ alloy system.

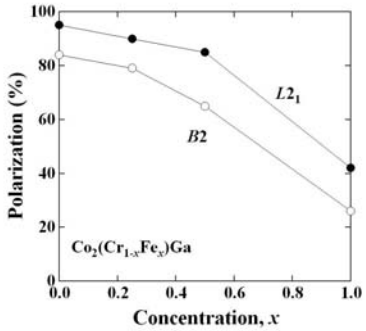

Fig. 8 Concentration dependence of the spin polarization ratio of the $L2_1$- and B2-type phases of the $Co_2(Cr_{1-x}Fe_x)Ga$ alloy system.

5. Co-base Superalloys:

The most fascinating heat-resistant alloys are the Ni-base superalloys, which are used, for example, in aircraft engines, industrial gas turbines, reactors, and the chemical industry. The main reason why Co-base alloys have not found widespread usage is their lower strength compared with that of Ni-base alloys, but they have been studied for a long time. With the development of Ni-base superalloys strengthened by the ordered γ' $Ni_3(Al, Ti)$ phase, the possibilities of precipitation hardening using geometrically close-packed phases that have the form of A_3B have been extensively investigated. Two types of geometrically close-packed phases have been reported in Co-base alloys: Co_3Ti with the $L1_2$ structure and ordered fcc Co_3Ta. Although the effect of various alloying elements on the stability and morphology of the γ' Co_3Ti phase has been investigated, the usefulness of the γ' phase is restricted to temperatures below 1023 K. In the case of Co_3Ta, the ordered fcc phase is metastable and readily converts to the stable hexagonal close-packed (hcp) structure Co_3Ta. Furthermore, the lattice parameter mismatches of these phases in Co-base alloys are usually more than 1.0%, which is not as useful for strengthening as the geometrically

close-packed phases in Ni-base superalloys, where mismatches typically vary from –0.1 to + 0.5%. Geometrically close-packed phase strengthening has thus not been used in commercial Co-base superalloys.

In determining the phase diagram of the Co-Al-W ternary system, we found a stable ternary compound with the $L1_2$ structure, which has the form $Co_3(Al, W)$, designated as γ'. Figure 9A shows a transmission electron micrograph of Co-9Al-7.5W (at%) annealed at 1173K for 72 hours after solution treatment at 1573K for 2 hours. The cuboidal phase homogeneously precipitates in the γ(A1) matrix, which is very similar to the morphology observed in Ni-base superalloys. The selected area electron diffraction pattern of the same sample is also shown in Fig. 9B, where the crystal structure of the γ' phase is confirmed as being the $L1_2$ ordered structure and the cuboidal γ' precipitates align along the <001> directions. The compositions of the matrix and that of the precipitate were determined using a field emission electron probe micro-analyzer (FE-EPMA). The composition of cuboidal precipitates observed in Fig. 9A is the ternary compound $Co_3(Al, W)$, where the composition of Al and W has an almost equiatomic ratio. In the geometrically close-packed A_3B compound, the stable Co_3W phase with the DO_{19} structure appears in the Co-W binary system. Although no stable compound of Co_3Al is formed in the Co-Al binary system, the formation of an ordered Co_3Al phase has been reported. Recently, the metastable Co_3Al phase with the $L1_2$ structure, which is formed in the Co-14at%Al alloy annealed at 873K for 24 hours, was observed by our group. It can be said, therefore, that metastable Co_3Al γ' is stabilized by alloying with W. Ternary compounds of $Co_3(Al, Cr)$ or $Co_3(Al, Mo)$ have not been reported.

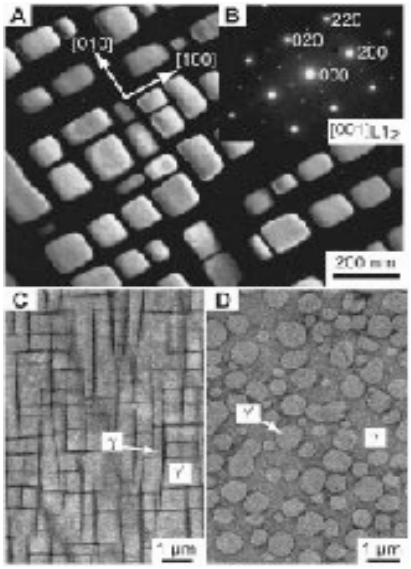

Fig. 9 Election micrographs of Co-9Al-7.5W alloy annealed at 1173 K for 72 hours. (**A**) Darkfield image. (**B**) Selected area diffraction pattern. (**C** and **D**) Field emission scanning electron micrographs of Co-8.8Al- 9.8W-2Ta (C) and Co-8.8Al-9.8W- 2Mo (D) annealed at 1273 K for 1 week.

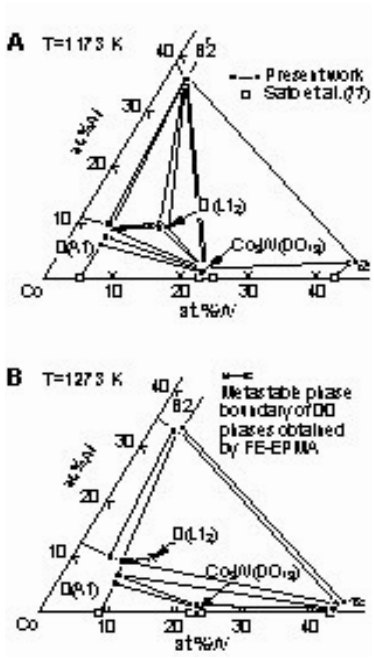

Fig. 10 Isothermal section diagrams of the Co-Al-W ternary system in the Co-rich portion at (**A**) 1173 K and (**B**) 1273 K.

Figures 10, A and B, show isothermal section diagrams determined experimentally in the present study, as well as recent data on the Co-W binary system at 1173 and 1273K, respectively. The γ' phase is stable at 1173K but metastable at 1273K. The thermal stability of the γ' phase and the effect of alloying were investigated by differential scanning calorimetry (DSC). Figure 11A shows the DSC curves on heating, where the solvus temperature was determined from the endothermic peak, as indicated by arrows. The DSC curve of Waspaloy [Ni-21Cr-2.5Mo-13Co-2.9Al-3.5Ti-0.3C (at%)], a widely used commercial Ni-base superalloy, is also shown. The solvus temperatures of the γ' phase in the Co-Al-W ternary system is ~ 1263K, which corresponds well with the phase diagram, as shown in Fig.10. The addition of Ta stabilizes the γ' phase such that the solvus temperature is ~ 1373K, and this value is higher than that of Waspaloy. The addition of Nb or Ti shows a similar effect. It can also be seen from Fig.11A that the melting temperatures of Co-Al-W-base alloys are ~1673K, which is 50 to 100K higher than those of Ni-base superalloys. Figure 11B shows the temperature variation of Vickers hardness of the γ+γ' structure for Co-9.2Al-9W and Co-8.8Al-9.8W- 2Ta aged at 1073K for 24 hours after solution treatment at 1573K for 2 hours. Aging treatment of Waspaloy was carried out at 1118K for 24 hours and 1033K for 16 hours after solution treatment at 1353K for 4 hours. The hardness of the γ+γ' structure of the Co-9.2Al-9W alloy is very similar to that of Waspaloy. The addition of Ta increases the hardness, which might be due to the stabilization of the γ' phase up to 1373K. The 0.2% compressive proof strengths of Co-9.2Al-9W and Co-8.8Al-9.8W-2Ta alloys are 473 and 674MPa at 1143K, respectively, as compared with 520MPa for the 0.2% tensile proof strength of Waspaloy. These data correspond well with the results for high-temperature hardness in Fig.11B.

We also identified a ternary compound, γ' $Ir_3(Al,W)$, with the $L1_2$ structure, which suggests that the Co-Ir-Al-W-base systems with γ+γ' $(Co,Ir)_3(Al,W)$ structures offer great promise as candidates for next-generation high-temperature materials.

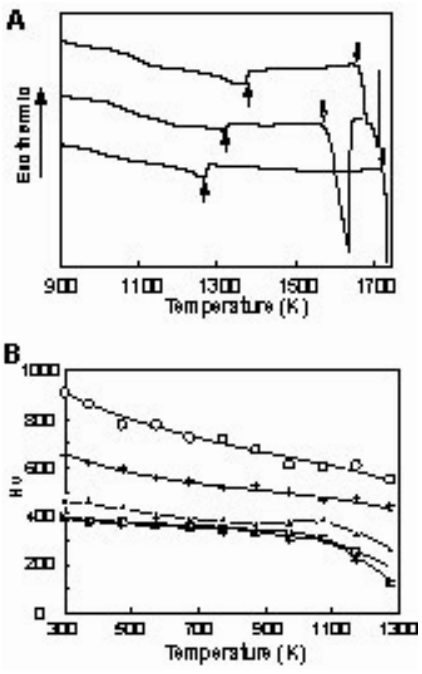

Fig. 11 (**A**) DSC curves. (Top) Co-8.8Al-9.8W-2Ta; (middle) Waspaloy; (bottom) Co-9.2Al-9W.
(**B**) High-temperature Vickers hardness. (○)Ir-20Co-10Al-10W, (+)Ir-10Al-10W (*)Co-9.2Al-9W, (▲)Co-8.8Al-9.8W-2Ta, (□) Waspaloy.

REFERENCES

1 K. Oikawa, G. W. Qin, T. Ikeshoji, R. Kainuma and K. Ishida, "Direct Evidence of Magnetically Induced Phase Separation in the fcc Phase and Thermodynamic Calculations of Phase Equilibria of the Co-Cr System", Acta. Mater., 50 (2002) 2223-2232.

2 K. Oikawa, G. W. Qin, O. Kitakami, Y. Shimada, K. Fukamichi and K. Ishida, "Magnetically Induced Two-phase Separation in Co-Ge and Co-Si Systems ", J. Mag. Mag. Mater., 239 (2002) 409-411.

3 K. Oikawa, G. W. Qin, S. Okamoto, O. Kitakami, Y. Shimada, K. Fukamichi and K. Ishida, "Thermodynamic Calculations of the Effect of B and Ta on Magnetically Induced Phase Separation in Co-Cr-Pt Alloys ", Appl. Phys. Lett., 80 (2002) 2704-2706.

4 K. Oikawa, F. W. Qin, M. Sato, O. Kitakami, Y. Shimada, J. Sato, K. Fukamichi and K. Ishida, "Magnetically Induced Phase Separation and Magnetic Properties of Co-Mo Hexagonal-close-packed Structure Thin Films", Appl. Phys. Lett., 83, (2003) 966-968.

5 K. Oikawa, G. W. Qin, M. Sato, S. Okamoto, O. Kitakami, Y. Shimada, K. Fukamichi, K. Ishida and T. Koyama, "Direct Observation of Magnetically Induced Phase Separation in Co-W-Sputtered Thin Films", Appl. Phys. Lett., 85, (2004), 2559-2561.

6 G. W. Qin, K. Oikawa, M. Sato, O. Kitakami, Y. Shimada, K. Fukamichi and K. Ishida, "Co-Mo and Co-Mo-Cr Alloy Thin Films Promising for Magnetic Recording", IEEE Trans. Mag., 41 (2005) 918-920.

7 J. Sato, K. Oikawa, R. Kainuma and K Ishida, "Experimental Verification of Magnetically Induced Phase Separation in αCo Phase and Thermodynamic Calculations of Phase Equilibria in the Co-W System", Mater Trans. 46, (2005) 1199-1207.

8 K. Oikawa, L. Wulff, T. Iijima, F. Gejima, T. Omori, A. Fujita, K. Fukamichi, R. Kainuma and K. Ishida, "Promising Ferromagnetic Ni-Co-Al Shape Memory Alloy System", Appl. Phys. Lett., 79 (2001) 3290-3292.

9 Y. Murakami, D. Shindo, K. Oikawa, R. Kainuma and K. Ishida, "Magnetic Domain Structures in Co-Ni-Al Shape Memory Alloys Studied by Lorentz Microscopy and Electron Holography.", Acta. Mater., 50 (2002) 2173-2184.

10 H. Morito, A. Fujita, K. Fukamichi, K. Oikawa, R. Kainuma and K. Ishida, "Mangetocrystalline Anisotropy in Single-Crystal Co-Ni-Al Ferromagnetic Shape-Memory Alloy", Appl. Phys. Lett., 81 (2002) 1657-1659.

11 A. Fujita, H. Morito, T. Kudo, K. Fukamichi, R. Kainuma, K. Ishida and K. Oikawa, "Magnetocrystalline Anisotropy in a Single-variant Co-Ni-Al Ferromagnetic Shape

Memory Alloy", Mater. Trans., 44, (2003) 2180-2183.
12 Y. Tanaka, T. Omori, K. Oikawa, R. Kainuma and K. Ishida, "Ferromagnetic Co-Ni-Al Shape Memory Alloys with β+α Two-Phase Strucutre.", Mater. Trans., 45 (2004) 427-430.
13 PJ. Brown, K. Ishida, R. Kainuma, T. Kanomata, K-U. Neumann, K. Oikawa, B. Ouladdiaf and K. R. A. Ziebeck, "Crystal Structures and Phase Transitions in Ferromangetic Shape Memory Alloys Based on Co-Ni-Al and Co-Ni-Ga", J. Phys. Condens. Mater., 17 (2005) 1301-1310.
14 Y. Tanaka, K. Oikawa, Y. Sutou, T. Omori, R. Kinuma and K. Ishida, “Martensitic transition and superelasticity of Co-Ni-Al ferromagnetic shape memory alloys with β＋γ two-phase structure”, Materials Science and Engineering, A 438-440 (2006), 1054-1060.
15 K. Ishikawa, R. Kainuma, I. Ohnuma, K. Aoki and K. Ishida, "Phase Stability of the X_2AlTi(X: Fe, Co, Ni and Cu) Heusler and B2-Type Intermetallic Compounds", Acta. Mater., 50 (2002) 2233-2243.
16 K. Kobayashi, R. Umetsu, R. Kainuma, K. Ishida, R. Oyamada, A. Fujita and K. Fukamichi, "Phase Separation and Magnetic Properties of Half-metal-type $Co_2Cr_{1-x}Fe_xAl$ Alloys", Appl. Phys. Lett., 85, (2004) 4684-4686.
17 R. Y. Umetsu, K. Kobayashi, R. Kainuma, A. Fujita, K. Fukamichi, K. Ishida and A. Sakuma, "Magnetic Properties and Band Structures of Half-metal-type Co_2CrGa Heusler Alloy ", Appl. Phys. Lett., 85, (2004) 2011-2013.
18 K. Kobayashi, R. Y. Umetsu, A. Fujita, K. Oikawa, R. Kainuma and K Ishida, " Magnetic Properties and Phase stability of Half-metal-type $Co_2Cr_{1-x}Fe_xGa$ Alloys", J. Alloys & Comp., 399, (2005) 60-63.
19 K. Kobayashi, R. Kainuma, K. Fukamichi, K. Ishida, "Phase equilibria and stability of B2 and $L2_1$ ordered phases in the vicinity of half-metallic composition of Co-Cr-Ga Heusler alloy system", Journal of Alloys and Compounds, 403 (2005)161-167.
20 R. Umetsu, K. Kobayashi, A. Fujita, K. Oikawa, R. Kainuma and K. Ishida, "Half-metallic Properties of $Co_2(Cr_{1-x}Fe_x)Ga$ Heusler Alloys", Phys. Rev., B72, (2005) 214412.
21 K. Kobayashi, R. Kainuma and K. Ishida, "Phase Separation and Stability of $L2_1$-Type Phase in $Co_2(Cr_{1-x}Fe_x)$ $(Ga_{1-y}Al_y)$ Alloys", Mater. Trans., 47, (2006) 20-24, No.1.
22 J. Sato, T. Omori, K. Oikawa, I. Ohnuma, R. Kainuma and K. Ishida, "Cobalt-Base High Temperature Alloys", Science, 312 (2006) 90-91.
23 H. Chinen, J. Sato, T. Omori, K. Oikawa, I. Ohnuma, R. Kainuma and K. Ishida, “New ternary compound Co_3(Ge, W) with $L1_2$ structure”, Scripta Materialia 56 (2006), 141-143.